Pericytes promote selective vessel regression to regulate vascular patterning

Nicole Simonavicius,[1] Matthew Ashenden,[1] Antoinette van Weverwijk,[1] Siân Lax,[2] David L. Huso,[3] Christopher D. Buckley,[2] *Ivo J. Huijbers,[1] *Helen Yarwood,[1] and *Clare M. Isacke[1]

[1]Breakthrough Breast Cancer Research Centre, Institute of Cancer Research, London, United Kingdom; [2]Rheumatology Research Group, School of Immunity and Infection, School of Clinical and Experimental Medicine, Medical Research Council Centre for Immune Regulation, Institute for Biomedical Research, College of Medical and Dental Sciences, University of Birmingham, Edgbaston, United Kingdom; and [3]Department of Molecular and Comparative Pathobiology and The Sidney Kimmel Comprehensive Cancer Center, Johns Hopkins Medical Institutions, Baltimore, MD

Blood vessel networks form in a 2-step process of sprouting angiogenesis followed by selective branch regression and stabilization of remaining vessels. Pericytes are known to function in stabilizing blood vessels, but their role in vascular sprouting and selective vessel regression is poorly understood. The endosialin (CD248) receptor is expressed by pericytes associated with newly forming but not stable quiescent vessels. In the present study, we used the *Endosialin*⁻/⁻ mouse as a means to uncover novel roles for pericytes during the process of vascular network formation. We demonstrate in a postnatal retina model that *Endosialin*⁻/⁻ mice have normal vascular sprouting but are defective in selective vessel regression, leading to increased vessel density. Examination of the *Endosialin*⁻/⁻ mouse tumor vasculature revealed an equivalent phenotype, indicating that pericytes perform a hitherto unidentified function to promote vessel destabilization and regression in vivo in both physiologic and pathologic angiogenesis. Mechanistically, *Endosialin*⁻/⁻ mice have no defect in pericyte recruitment. Rather, endosialin binding to an endothelial associated, but not a pericyte associated, basement membrane component induces endothelial cell apoptosis and detachment. The results of the present study advance our understanding of pericyte biology and pericyte/endothelial cell cooperation during vascular patterning and have implications for the design of both pro- and antiangiogenic therapies. (*Blood*. 2012;120(7):1516-1527)

Introduction

The expansion of existing blood vessels, known as angiogenesis, is a critical process that occurs in response to an insufficient supply of nutrients and oxygen during development and tissue regeneration. The deregulated generation and abnormal remodeling of blood vessels can promote the expansion of tumors or fail to restore tissue oxygenation adequately, contributing to ischemic disease progression (eg, in diabetic retinopathy). Therefore, the identification of the cellular and molecular targets for therapeutic strategies to influence vascular network formation and remodeling is of considerable clinical importance.[1,2] Angiogenesis is initiated in response to local production of proangiogenic factors, in particular VEGF-A, which promote new vascular sprout formation by the induction and migration of leading tip cells and by stimulating the proliferation of neighboring stalk cells. In addition, VEGF-mediated regulation of the Delta-like 4/Notch1 signaling pathway ensures the correct spatiotemporal coordination of tip versus stalk cell specialization required for organized patterning of new vascular networks.[3] Subsequent to sprouting angiogenesis, the initial vascular plexus is remodeled extensively. Key to this remodeling is the pruning of unwanted capillaries through selective branch regression. The remaining vessels mature and are stabilized, which marks the end of vessel plasticity and reflects the quiescent state of the new hierarchical vascular network. With the exception of the complete regression of the hyaloid vessels during development,[4,5] the detailed mechanisms of vascular pruning are poorly understood.

Blood vessels consist of 2 interacting cell types, endothelial cells and surrounding mural cells. Pericytes are mural cells that share a common basement membrane with endothelial cells, where they communicate with each other via physical contact and paracrine signaling pathways.[6-8] It is known that interactions between pericytes and endothelial cells are required for vessel survival, maturation, and stabilization, and the importance of the Ang1-Tie2 paracrine signaling pathway in this process has been documented extensively.[9,10] In keeping with this, it has been demonstrated in mature quiescent vessels in both mouse models and human disease states that disruption of the pericyte-endothelial cell interactions leads to destabilization of the then-unprotected vessels, which revert to a more plastic state and undergo widespread regression.[11-13]

The determination of the function of pericytes in early vascular patterning events, including sprouting angiogenesis and vascular pruning, has been hampered, at least in part, by the fact that pericytes constitute a heterogeneous population of cells that lack adequate and specific markers. For example, using α-smooth muscle actin (αSMA) to identify pericytes in the developing retina, it was suggested that pericyte coverage occurs only in the later stages of network formation associated with stabilizing and mature vessels and that the lack of pericyte coverage defines a vascular plasticity window.[11] However, more recent studies using panels of pericyte markers have shown that pericytes are already abundant in actively sprouting and remodeling vascular plexi, so their presence

per se does not mark vessel stability.[12,14-17] This finding highlights the need to investigate the relationship of the mechanistic contribution of this early pericyte investment to physiologic and pathologic angiogenesis and vascular remodeling.

Endosialin (CD248) is a type I transmembrane glycoprotein the expression of which in the vasculature is restricted to pericytes. Moreover, endosialin is expressed on newly forming vessels in developing tissues and a wide variety of tumors, but its expression is strongly down-regulated on resting, adult vessels.[18-23] Given this unique expression pattern, in the present study we investigated both developmental and tumor angiogenesis in wild-type and *Endosialin*^{−/−} mice to address a fundamental and unexplored biologic question: do pericytes have active functions during sprouting angiogenesis and vascular pruning?

Methods

Cells and Abs

Immortalized mouse skin endothelial cells (sEND) were cultured in Dulbecco's modified Eagle's medium (DME) supplemented with 10% FCS and 2mM L-glutamine. For transfection with siRNA oligonucleotides, sEND cells were plated in antibiotic-free medium and transfected the next day with Dharmacon SMARTpool siRNAs against mouse urokinase plasminogen activator (uPA; *Plau*: M-060180-00) and/or urokinase plasminogen activator receptor (uPAR; *Plaur*: M-061572-01) or nontargeting control SMARTpool siRNA (D-001206-13) at a final concentration of 100nM using oligofectamine (Invitrogen) in serum-free medium for 4 hours before replacement with full growth medium. For protease inhibitor treatment, sEND cells were cultured for 48 hours in the presence of 25 μg/mL of amiloride (Merck) or 400 U/mL of aprotinin (American Diagnostica). Human umbilical cords were donated by the Department of Obstetrics, Queen Charlotte's Hospital (London, United Kingdom). The use of human endothelial cells conforms to the principles outlined in the Declaration of Helsinki and was approved by the Hammersmith Hospital's (London, United Kingdom) research ethics committee (reference number 06/Q0406/21). Human umbilical vein endothelial cells (HUVECs) were isolated as described previously[24] and cultured in M199 medium (Sigma-Aldrich) supplemented with 20% FCS and 10 μg/mL of heparin (Sigma-Aldrich), 20 μg/mL of endothelial cell growth supplement (Serotech), and 2mM L-glutamine on 0.1% gelatin (Sigma-Aldrich)–coated dishes. For VEGF-A stimulation, 2×10^4 HUVECs were cultured on endosialin extracellular domain (ES-Fc; amino acids 1-369)– or control human IgG₁ (hFc)–coated 6-well plates for 48 hours, serum starved for 2 hours, and stimulated with 40 ng/mL of VEGF-A164 (R&D Systems) for the indicated times. HUVECs were used between passages 2 and 5.

The polyclonal anti-endosialin Ab P13 has been described previously.[18] Anti–mouse NG2 polyclonal Ab was a kind gift of Bill Stallcup (Burnham Institute for Medical Research, La Jolla, CA). The following Abs and reagents were obtained commercially: mouse collagen IV (Millipore or Acris Antibodies), mouse fibronectin (Abcam), FITC–annexin V, ICAM-2 (clone 3C4) and mouse CD31 (clone MEC 13.3; BD Biosciences), mouse endomucin (Santa Cruz Biotechnology), αSMA, FITC-hFc, Cy3-hFc, α-tubulin, and phospho-ERK1/2 (Sigma-Aldrich), VEGFR2, Tyr1175-phosphorylated VEGFR2, ERK1/2, and activated caspase-3 (Cell Signaling Technology), FITC-isolectin B4 (Vector Laboratories), anti-glial fibrilliary acidic protein (GFAP), Alexa Fluor 488–isolectin B4, Alexa Fluor–conjugated secondary Abs (Invitrogen), and HRP-conjugated secondary Abs (Jackson ImmunoResearch Laboratories).

Mice

Endosialin^{−/−} mice[25] were backcrossed from a mixed 129/SvJ background into the C57BL/6 background. All procedures were in accordance with United Kingdom Home Office legislation.

Microscopy

Fluorescent images were collected sequentially in 3 or 4 channels on a Leica Microsystems TCS-SP2 or Zeiss LSM 710 confocal microscope. Within each experiment, all images were taken at the same settings. Unless otherwise indicated, a series of 0.5- to 1-μm optical sections were collected and the maximum projections are shown in the figures. Images were exported from the Leica or Zeiss Zen software into Adobe Photoshop Version 10.0.1 software. Phase contrast images were collected on an Olympus IX70 microscope.

Isolation and immunostaining of mouse retina

Retinal whole mounts were prepared as follows. After 5 minutes of fixation in 4% paraformaldehyde, the sclera was dissected in 2× PBS and the lens and vitreous removed. The retinas were fixed in 4% paraformaldehyde for 1 hour and then permeabilized in 2× concentrated PBS/2% FCS/0.5% Tween 20/3% Triton X-100 for 1 hour. Immunostaining with primary Abs was performed overnight at 4°C. The following day, retinas were washed 2 times for 5 minutes each in PBS and incubated with secondary Abs for 3-5 hours at 4°C. Retinas were mounted in 8 μL of Vectashield (Vector Laboratories) in CoverWell Imaging chambers (Stratagene) and images captured using 10× (HCPLAPOCS NA 0.4; Leica or EC Plan-Neofluar NA 0.3; Zeiss), 20× (HCPLAPOCS NA 0.7; Leica or EC Plan Neofluar NA 0.5; Zeiss), or 40× (HCXPLAPO NA 1.25; Leica or EC Plan Neofluar NA 1.3; Zeiss) lenses. To measure vessel density, images were changed into gray scale and quantified using either the Metamorph Version 7.5 software (Molecular Devices) "angiogenesis tube formation tool" or branch points were counted manually as described previously.[26] For P2-P4 retinas, 4 fields of view (440 μm × 440 μm; Figure 2A boxes and supplemental Figure 3A, available on the *Blood* Web site; see the Supplemental Materials link at the top of the online article) per retina representing the central capillary plexus were quantified. For P7 retinas, ≥ 4 fields of view (277 μm × 277 μm) were collected in 5 different areas of the retina, as illustrated in supplemental Figure 4. For quantification of vessel density in the sprouting plexus (Figure 4A asterisk), 8 fields of view (157 μm × 157 μm) were analyzed. Retinal expansion was measured in low-power Adobe Photoshop images taken with a 5× lens, and are represented as the distance migrated from the center of the optic disc as a percentage of the retinal diameter. To quantify the number of empty sleeves (collagen IV positive and isolectin B4 negative) and apoptotic vessels (defined as those in which the endothelial cells had intracellular activated caspase-3 staining), ≥ 4 micrographs (515 μm × 515 μm) were taken in the remodeling plexus.

Aortic ring outgrowth assay

Assays were performed as described previously.[27] Briefly, thoracic aortae from 6- to 12-week-old 129/SvJ mice were dissected, cleaned from fatty tissue, transversely cut into rings, and incubated overnight in serum-free OptiMEM medium (Invitrogen) at 37°C in 8% CO_2. The next day, rings were mounted in 60 μL of 1.1 mg/mL acid-solubilized rat tail type I collagen (BD Biosciences) in DME with 1 ring per well of a 96-well plate. After collagen polymerization, 180 μL of DME plus 2.5% FCS (Autogen Bioclear) and 30 ng/mL of VEGF-A164 were added. The culture medium was changed every 48 hours. After 6 days in culture, rings were fixed for 1 hour in 4% paraformaldehyde, permeabilized for 30 minutes with 0.5% Triton X-100, and, where indicated, immunostained. Rings were mounted in 8 μL of Vectashield in CoverWell Imaging chambers. For phase-contrast microscopy, 4 or 5 images per aortic ring (representing the entire aortic ring) were taken with a 10× (PhC, c plan, NA 0.15) lens of the Olympus IX70 microscope. Images were imported into Adobe Photoshop and sprout number, length, and branch points measured.

Tumor xenografts

B16-F0 melanoma cells (5×10^5) resuspended in 100 μL sterile PBS were injected subcutaneously into C57BL/6 *Endosialin*^{+/+} or *Endosialin*^{−/−} mice. Tumors were harvested after 7 or 14 days, fixed overnight in 4% paraformaldehyde, paraffin embedded, and sections cut at 3 levels (25%, 50%, and 75%) through the tumor. To quantify vessel density and the

number of collagen IV–positive, endomucin-negative empty sleeves, $\geq$ 6 micrographs per section with a field size of 750 μm $\times$ 750 μm were taken in the nonnecrotic areas.

Fc constructs

Soluble Fc constructs (illustrated in supplemental Figure 8A) contained the C-type lectin-like domain, the sushi domain, and the 3 EGF repeats of the mouse ES-Fc or the CD44 extracellular domain containing the R41A mutation to prevent hyaluronan binding (CD44-Fc).[28] Fc constructs were expressed and purified as described previously.[18] Endotoxin levels as measured using the kinetic LAL turbidimetric assay (Associates of Cape Cod International) were < 0.1 EU of endotoxin/μg. hFc was purchased from Sigma-Aldrich. To coat plates, wells were incubated with 1 μg/mL of ES-Fc, CD44-Fc, or hFc in 0.05M carbonate/bicarbonate buffer overnight at 4°C. Plates were washed and coated with 0.1% gelatin (BD Biosciences). For binding assays, aortic rings cultured for 6 days were incubated without fixation with 10 μg/mL of ES-Fc, CD44-Fc, or hFc for 1 hour at 37°C in DME. Frozen embryos were fixed with 4% paraformaldehyde and incubated with 50 μg/mL of ES-Fc overnight at 4°C. After fixation, Fc construct binding was detected with FITC–anti-Fc or Cy3–anti-Fc and cells counterstained with Alexa Fluor 555–phalloidin and DAPI. ES-Fc binding was quantified using the histogram quantification tool of the Leica confocal software. The mean number of pixels measured in the 488 channel (ES-Fc binding) was normalized against the number of cells (ie, the mean number of pixels retrieved from the DAPI staining: the 405 channel).

Apoptosis and cell detachment

For annexin V staining, HUVECs or C3H/10T1/2 mouse embryonic mesenchymal cells were cultured for 48 hours, serum starved for 2 hours, and then incubated with 20 ng/mL of VEGF-A164 plus 50 μg/mL of ES-Fc or hFc for 3 hours. Cells were trypsinized, washed twice with PBS, stained with FITC–annexin V and propidium iodide for 15 minutes at room temperature, and analyzed in an LSRII FACS analyzer (BD Biosciences). In detachment assays, HUVEC were cultured for 48 hours, incubated in serum-free medium for 2 hours, and then treated with medium containing 10 ng/mL of VEGF-A164 and 2% FCS in the presence of 100 μg/mL of hFc, ES-Fc, or CD44-Fc.

Statistical analyses

The Prism Version 5 statistical package (GraphPad) was used for statistical analyses. Unless otherwise stated, numerical data are expressed as means $\pm$ SEM. Experiments were analyzed with the unpaired Student t test. All tests were 2-tailed with a confidence interval of 95%. Where multiple comparisons were made, 1-way ANOVA with Bonferroni posttest and a confidence interval of 95% was used.

Results

Endosialin-deficient mice have increased retinal vessel density

To investigate the role of endosialin in sprouting angiogenesis and vascular remodeling, initially we used the postnatal mouse retina model of developmental angiogenesis. During the first 8 days after birth, angiogenic blood vessels emerge from the optic disc and spread radially around the back of the retina. The advantage of this model is that it allows examination of sprouting angiogenesis, vascular remodeling, and maturation in a single preparation.[29] In wild-type mice, low-level expression of endosialin is detected on pericytes as early as postnatal day 2 (P2; Figure 1A). This expression increases during the first few days of retinal development so that by P4, endosialin is expressed strongly (Figure 1A-B) and its expression remains elevated throughout the later stages of retinal development (supplemental Figure 1). Endosialin expression is detected on pericytes throughout the developing superficial

vascular plexus from the optic disc to the retinal periphery (Figure 1 and supplemental Figure 1), and at all postnatal stages examined, all pericytes coexpressed endosialin and the alternative pericyte marker NG2 (Figure 1C and supplemental Figure 2). Consistent with previous results,[18,20-22,30] no endosialin expression was detected on the vascular endothelial cells (Figure 1D).

Examination of the central capillary plexus adjacent to the optic disc of C57BL/6 $Endosialin^{+/+}$, $Endosialin^{+/-}$, and $Endosialin^{-/-}$ mice revealed a clear increase in retinal vessel density in $Endosialin^{-/-}$ retinas (Figure 2). This phenotype was also observed in 129/SvJ mice (supplemental Figure 3), indicating a strain-independent effect. Quantification of vessel density using either the angiogenesis tube formation tool (Figure 2B and supplemental Figure 3B) or manual counting of the vascular branch points (Figure 2C) showed a significant increase in vascular density at P3 and P4 and a clear trend at P7 in the $Endosialin^{-/-}$ retinas. This trend in increased vessel density was also observed further out in the $Endosialin^{-/-}$ P7 retinas (supplemental Figure 4 regions 2 and 3), but not in the outer regions (regions 4 and 5). This phenotype was not because of failure of pericyte recruitment or distribution, because NG2 staining revealed no detectable difference in pericyte coverage between the $Endosialin^{+/+}$, $Endosialin^{+/-}$, and $Endosialin^{-/-}$ retinas (Figure 2D and supplemental Figure 3A).

Loss of endosialin leads to a defect in aortic ring vascular outgrowths

To assess whether the vascular defects associated with the loss of $Endosialin$ were recapitulated in an independent model, we examined angiogenesis from ex vivo aortic rings of adult animals. In wild-type aortic ring explants, the vascular sprouts contained an inner core of isolectin B4-positive endothelial cells surrounded by closely associated endosialin-positive pericytes (Figure 3A). Within 6 days of explant culture, VEGF-dependent outgrowths of capillary sprouts from the aortic rings were observed in both wild-type and $Endosialin^{-/-}$ mice. There was no significant difference in the number of sprouts emanating from the rings; however, the $Endosialin^{-/-}$ aortae revealed a markedly different capillary outgrowth pattern (Figure 3B and supplemental Figure 5). Sprouts were longer in length, had an increased number of branch points, and showed a more disorganized outgrowth pattern. As observed in the retinal vasculature, lack of endosialin protein did not prevent pericyte recruitment to the aortic ring capillary sprouts (data not shown).

Loss of endosialin results in impaired selective vessel regression

The increased vessel density observed in retinas of $Endosialin^{-/-}$ mice (Figure 2 and supplemental Figure 3) may occur as a result of increased sprouting activity at the vascular front and/or reduced pruning of the initial primitive plexus through impaired selective vessel regression. To address the former, a detailed analysis of the sprouting plexus was undertaken. In the absence of endosialin, no difference was detected in the number of tip cells or in the extent and alignment of tip cell filopodia with the underlying astrocytic network (Figure 4A) identified by expression of GFAP and low level expression of NG2 (supplemental Figure 6). Further, in the area situated immediately behind the leading tip cells (Figure 4A asterisk), there was no significant difference in vessel density between $Endosialin^{+/+}$ and $Endosialin^{-/-}$ 129/SvJ mice or between $Endosialin^{+/+}$, $Endosialin^{+/-}$, and $Endosialin^{-/-}$ C57BL/6 mice (Figure 4B), indicating that sprouting activity is not affected
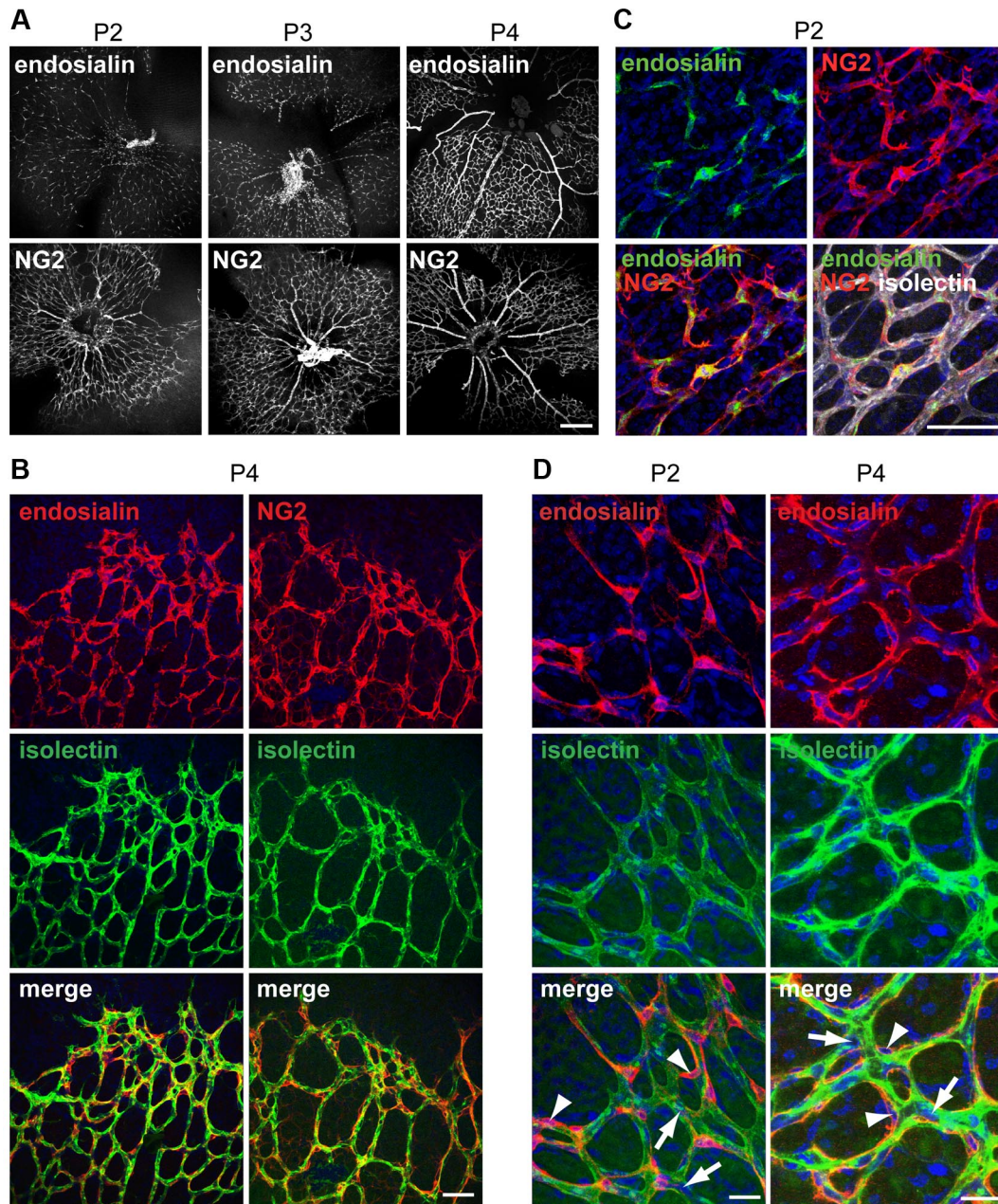
Figure 1. Expression of endosialin in the postnatal mouse retina. Whole-mount retinas from P2, P3, and P4 wild-type 129/SvJ mice were stained as follows. (A) Anti-endosialin or anti-NG2 polyclonal Ab followed by Alexa Fluor 555 anti–rabbit Ig. Scale bar indicates 250 μm. (B) Anti-endosialin or anti-NG2 polyclonal Ab and Alexa Fluor 555 anti–rabbit Ig (red), FITC–isolectin B4 (green), and DAPI (blue). Scale bar indicates 50 μm. (C) Anti-endosialin mAb 3K2L (supplemental Figure 2) and anti–rat Ig (green), anti-NG2 and anti–rabbit Ig (red), FITC–isolectin B4 (white), and DAPI (blue). Scale bar 50 μm. (D) Anti-endosialin polyclonal Ab followed by Alexa Fluor 555–anti–rabbit Ig (red), FITC–isolectin B4 (green), and DAPI (blue). Endosialin expression is detected on pericytes (arrowheads) but not endothelial cells (arrows). Scale bar indicates 25 μm.

by loss of endosialin. In keeping with this notion, no significant difference in radial expansion of the superficial vascular plexus was observed between *Endosialin*$^{+/+}$ and *Endosialin*$^{-/-}$ 129/SvJ mice or between *Endosialin*$^{+/+}$, *Endosialin*$^{+/-}$, and *Endosialin*$^{-/-}$ C57BL/6 mice (Figure 4C).

To investigate directly whether the *Endosialin*$^{-/-}$ retinas have an impairment in selective vessel regression, we examined the remodeling plexus. Regressing endothelial cells leave empty sleeves of matrix deposits rich in the basement membrane component collagen IV.[31-33] In the remodeling plexus, empty sleeves (collagen IV positive and isolectin B4 negative) were clearly detected in wild-type retinas and were prominent adjacent to the

arteries and in the more mature region of the plexus proximal to the optic nerve (Figure 5A arrowheads) and denote regression profiles. In *Endosialin*$^{+/-}$ and *Endosialin*$^{-/-}$ retinas, there were significantly fewer empty sleeves detected (Figure 5A), indicating defective vessel regression. Therefore, the *Endosialin*$^{-/-}$ phenotype is consistent with normal branching but defective regression of neocapillaries, leading to increased vascular density in the remodeling plexus. Consistent with many of the defects detected in retinal angiogenesis,[34-36] the endosialin phenotype resolves over time. The increased vascular density was still observed in P7 *Endosialin*$^{-/-}$ retinas in the remodeling plexus adjacent to the optic nerve (region 1) and further out (regions 2 and
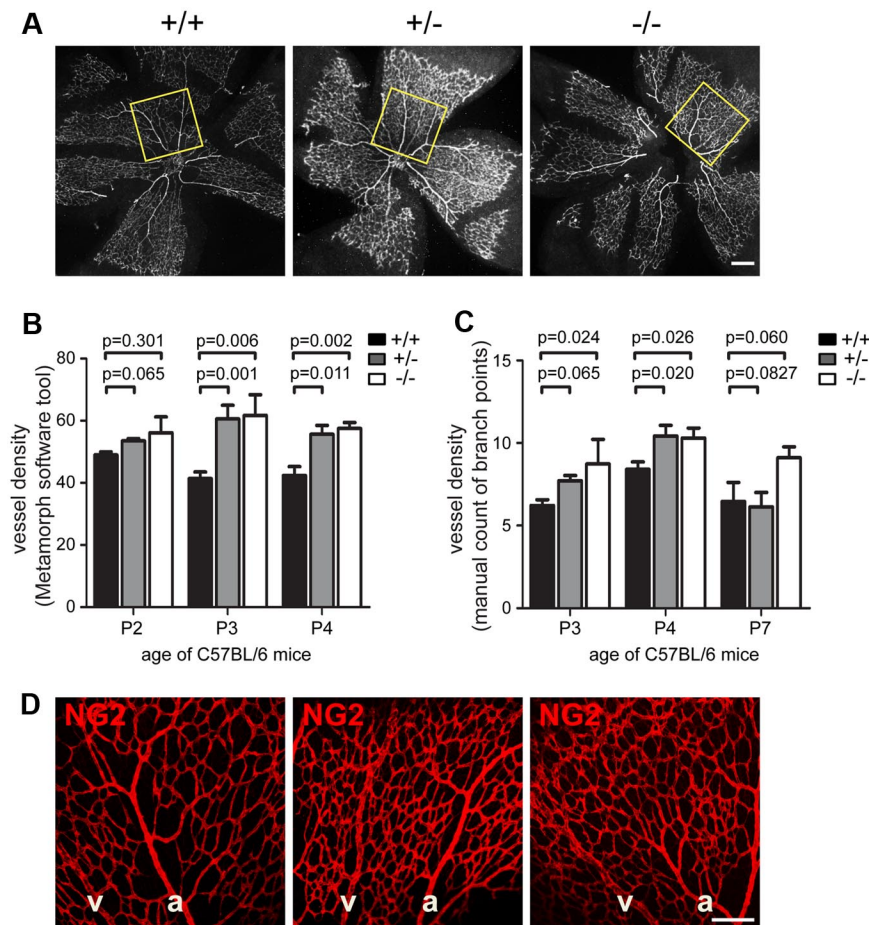
Figure 2. Loss of *Endosialin* results in increased vessel density. Retinas from littermate *Endosialin*^{+/+}, *Endosialin*^{+/−}, and *Endosialin*^{−/−} C57BL/6 mice were stained with FITC–isolectin B4 and NG2 followed by Alexa Fluor 555–anti–rabbit Ig. (A) Low-power images of P4 retinas with box indicating the field of view in the central capillary plexus analyzed for quantification of vessel density in panels B and C. (B) Quantification of vessel density (Metamorph software tool)/100 μm² ± SEM. (C) Quantification of vessel density (manual counting of branch points)/100 μm² ± SEM. *Endosialin*^{+/+}: P2, n = 5; P3, n = 7; P4, n = 5; P7, n = 3. *Endosialin*^{+/−}: P2, n = 5; P3, n = 4; P4, n = 5; P7, n = 7. *Endosialin*^{−/−}: P2, n = 4; P3, n = 4; P4, n = 5; P7, n = 5. (D) Confocal images of P4 retinas to illustrate no difference in NG2-positive pericyte coverage in *Endosialin*^{+/+}, *Endosialin*^{+/−}, and *Endosialin*^{−/−} mice. a indicates arteries; and v, veins. Scale bar indicates 200 μm.

3; supplemental Figure 4). However, by P21, all 3 plexi (superficial, intermediate, and deep) were present with no detectable abnormalities in the *Endosialin*^{−/−} mouse (data not shown), indicating that loss of endosialin reduces the speed of pruning rather than causing an inability to prune.

To assess whether pericytes also function to promote vascular pruning during pathologic angiogenesis, we next examined the vasculature of B16-F0 melanoma cells grown as tumors in *Endosialin*^{+/+} and *Endosialin*^{−/−} mice. Staining with the endothelial marker endomucin revealed that the *Endosialin*^{−/−} tumor vasculature showed an increased number of smaller vessels and a reduced number of larger vessels compared with the vasculature of tumors grown in *Endosialin*^{+/+} mice (Figure 5B). This aberrant vascular pattern is consistent with previous reports using different tumor models in endosialin-deficient mice.[25,37] In keeping with our findings in the developing retina and ex vivo aortic ring outgrowths, there was no overt defect in pericyte recruitment in the *Endosialin*^{−/−} tumor vasculature as monitored by SMA and NG2 staining (supplemental Figure 7A). There was a significant decrease in the number of collagen IV–positive, endomucin-negative empty sleeves in the *Endosialin*^{−/−} tumor vasculature (Figure 5B), demonstrating that the pruning defect observed in physiologic angiogenesis also underlies the aberrant vascular phenotype in tumors in *Endosialin*^{−/−} mice. No differences were detected in subcutaneous tumor growth or overall levels of tumor hypoxia and necrosis (supplemental Figure 7B). These latter observations are in agreement with previous studies showing that tumor size was not impaired in *Endosialin*^{−/−} mice after subcutaneous[25] or intracranial[37] tumor cell inoculation. However, when tumor cells were

implanted into the liver or onto the serosal surface of the large intestine, reduced tumor growth was observed in *Endosialin*^{−/−} mice.[25] These combined tumor studies suggest site specificity in the ability of the vasculature to compensate functionally for loss of endosialin expression.

Interaction of endosialin with the vascular basement membrane

To investigate the mechanism by which pericyte-expressed endosialin is able to promote vessel pruning, we generated a soluble endosialin-Fc construct (supplemental Figure 8A ES-Fc) to ascertain the localization of endosialin ligand(s) in vivo. ES-Fc bound the basement membrane associated with the abluminal surface of endothelial cells in cryosections of embryonic day 15 mouse brain (Figure 6A arrowhead); however, it was notable that no binding was detected in the basement membrane on the basal side of the associated pericytes (Figure 6A arrow). An equivalent pattern of staining was observed in wild-type aortic vascular outgrowths (Figure 6B). ES-Fc binding detected in in vivo and ex vivo specimens was specific and not mediated by the Fc domain, because no binding was observed with a control Fc construct[28] (Figure 6B CD44-Fc). In cell-free assays, it has been reported that endosialin binds to the extracellular matrix components fibronectin and collagen IV, but not to vitronectin or laminin.[38] In the present study, double labeling of the aortic ring cultures revealed that fibronectin was present in both endothelial cell- and pericyte-associated basement membrane and the associated fibroblasts (Figure 6C), indicating that endosialin does not bind universally to

Figure 3. Loss of *Endosialin* results in aberrant vascular sprouts in the aortic ring outgrowth assay. Thoracic aortae were dissected from *Endosialin*^{+/+} or *Endosialin*^{−/−} 129/SvJ mice, embedded in a collagen I matrix and cultured for 6 days in the presence of VEGF-A. (A) Fixed wild-type aortae stained with FITC–isolectin B4 (green) and anti–mouse Endosialin Ab followed by Alexa Fluor 555–anti–rabbit Ig (red). Nuclei were counterstained with DAPI. Image shows a vascular sprout with expression of Endosialin on pericytes (arrowheads) but not endothelial cells (arrows). Scale bar indicates 25 μm. (B) Phase-contrast images illustrating increased vascular branching in *Endosialin*^{−/−} outgrowths (arrows). Scale bar indicates 200 μm. Quantification of aortic ring vascular sprout number (n = 12), sprout length (n = 5), and branch point number (n = 5) per aortic ring. Data shown are means ± SEM.
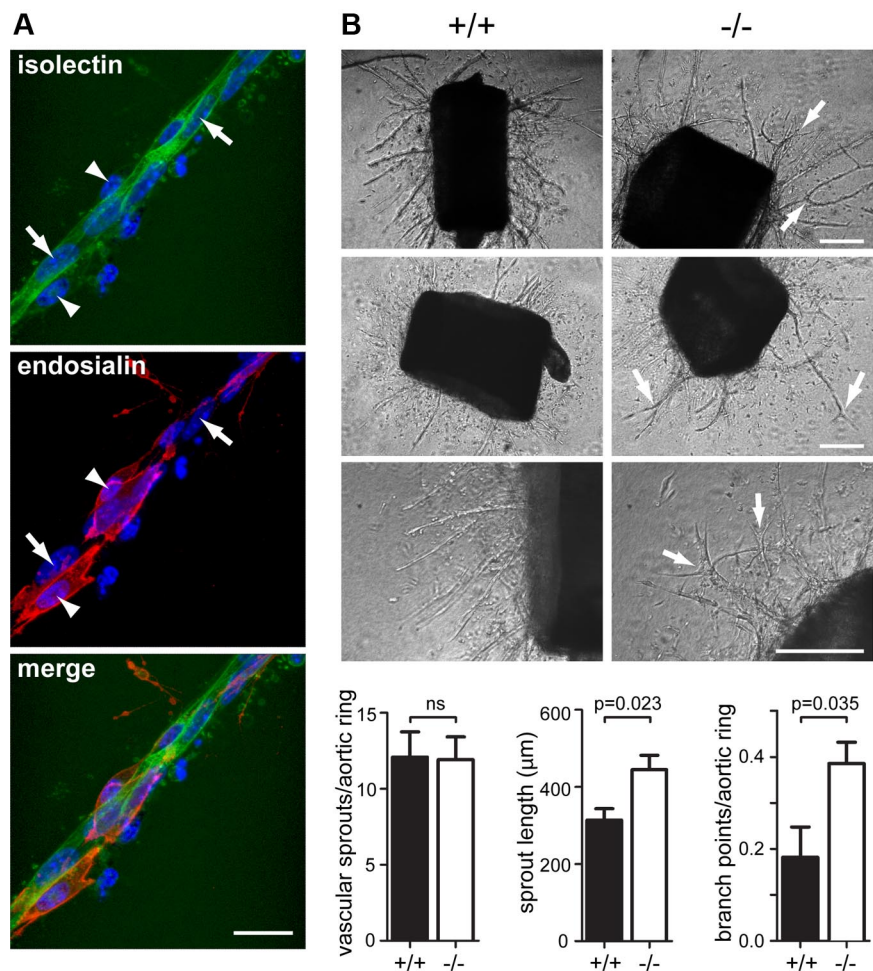
fibronectin in vivo. This observation was confirmed in vitro, where ES-Fc binding was restricted to extracellular matrix components deposited by endothelial cells (supplemental Figure 8B-D). No binding was detected to the extracellular matrix deposited by other cell types despite abundant fibronectin production by all cultured cells examined. Binding to the endothelial cell matrix in vitro was again specific to ES-Fc with no binding of CD44-Fc detected (supplemental Figure 8D).

During angiogenesis and subsequent vessel remodeling, the vascular basement membrane undergoes extensive reorganization that is known to regulate pericyte-endothelial cell interactions, and key to these events is the activity of proteases.[39,40] Treatment of sEND cells with amiloride and/or aprotinin impaired ES-Fc binding to the endothelial cell extracellular matrix (Figure 6D). Because amiloride and aprotinin act as inhibitors of the uPA/uPAR/plasminogen pathway, sEND cells were treated with siRNA oligonucleotides against uPA and/or uPAR. Control siRNA treatment had no effect on ES-Fc binding, but down-regulation of either uPA or uPAR resulted in decreased binding with a further significant blockade observed in cells treated with uPA and uPAR siRNAs together (Figure 6E). These data indicate a mechanism by which endosialin activity could be localized by endothelial cell proteases.

Endosialin promotes endothelial cell apoptosis

Changing levels of pro- and antiangiogenic factors, in particular, decreasing levels of VEGF, play a key role in determining vascular

pruning during angiogenesis.[1] To examine whether endosialin modulates the response of endothelial cells to VEGF-A, HUVECs were plated onto ES-Fc–coated dishes to mimic the presentation of endosialin by pericytes. Cells cultured on ES-Fc, compared with control hFc, showed attenuated VEGF-mediated signaling as monitored by VEGFR2 Tyr1175 and ERK1/2 phosphorylation, but no reduction in total VEGFR2 expression (Figure 7A). At 24 hours, the attenuated signaling of cells plated onto ES-Fc translates into a significant decrease in cell viability (Figure 7B). To investigate whether endosialin could promote endothelial cell apoptosis, serum-starved HUVECs were treated with VEGF-A and soluble ES-Fc. FACS analysis revealed a 65% increase in annexin V–positive and annexin V/propidium iodide double-positive HUVECs after 3 hours in the presence of ES-Fc compared with hFc control (Figure 7C) or CD44-Fc control (data not shown). Treatment with ES-Fc did not promote apoptosis in cultured 10T1/2 pericyte-like cells (Figure 7C). Consistent with this promotion of endothelial cell apoptosis, HUVECs cultured in the presence of soluble ES-Fc, but not control CD44-Fc or hFc, showed increased cell detachment by 8 hours (Figure 7D). To confirm that the increased apoptosis and cell detachment observed in vitro reflected the defect in vessel pruning observed in vivo, retinas from *Endosialin*^{+/+}, *Endosialin*^{+/−}, and *Endosialin*^{−/−} mice were stained for collagen IV, activated caspase-3, and isolectin B4. In the *Endosialin*^{+/+} remodeling plexus, endothelial cells with intracellular activated caspase-3 staining were readily detected and this loss of endothelial cells was clearly associated with the formation of
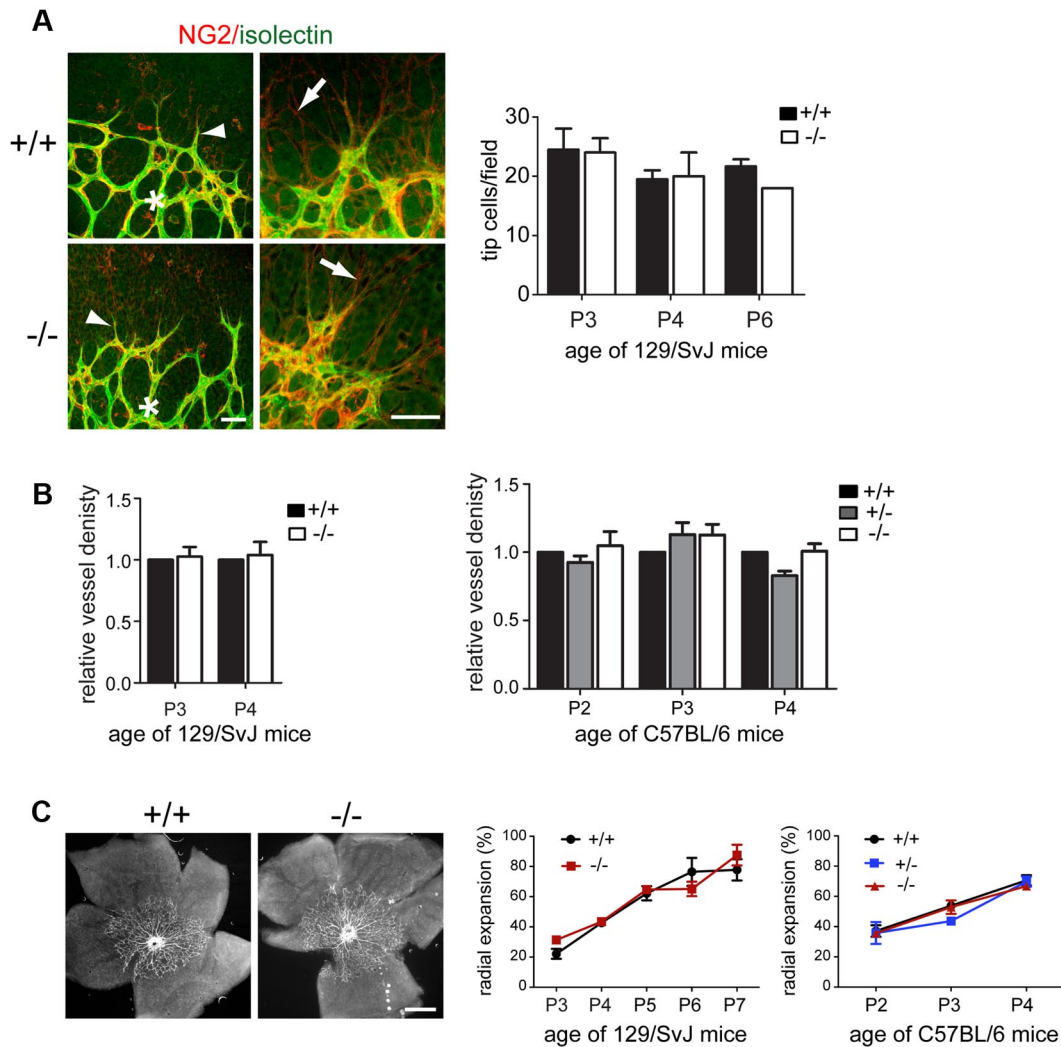
Figure 4. Sprouting angiogenesis is not affected by loss of _Endosialin_. Retinas were stained with FITC–isolectin B4 (green) and NG2 followed by Alexa Fluor 555–anti–rabbit Ig (red). (A) Confocal images of P3 _Endosialin_[+/+] and _Endosialin_[−/−] 129/SvJ retinas taken at the sprouting front of the expanding vasculature showing no difference in the alignment of tip cell filopodia (arrowheads) with the underlying NG2-positive astrocyte network (arrows). Scale bars indicate 50 µm. Graph shows quantification of tip cell number. (B) Vessel density in the sprouting plexus was analyzed immediately behind the sprouting front (indicated by asterisk in panel A). Graph shows quantification of vessel density at the sprouting front ± SEM. No significant difference was observed at any time point. For panels A and B, 129/SvJ _Endosialin_[+/+]: P3, n = 6; P4, n = 3; _Endosialin_[−/−] P3, n = 8; P4, n = 4. C57BL/6 _Endosialin_[+/+]: P2, n = 3; P3, n = 7; P4, n = 4. _Endosialin_[+/−] P2, n = 4; P3, n = 4; P4 = 4. _Endosialin_[−/−]: P2, n = 2; P3, n = 3; P4, n = 7. (C) Left panels show representative low-power images of 129/SvJ P3 retinas. Scale bar indicates 500 µm. Right panels show quantification of the radial expansion of the vascular plexus at each time point ± SD. No significant difference was observed at any time point. 129/SvJ; _Endosialin_[+/+]: P3, n = 3; P4, n = 4; P5, n = 4; P6, n = 4, P7, n = 2. _Endosialin_[−/−]: P3, n = 2; P4, n = 2; P5, n = 3; P6, n = 4, P7, n = 3. C57BL/6; _Endosialin_[+/+]: P2, n = 3; P3, n = 3; P4, n = 3. _Endosialin_[+/−]: P2, n = 4; P3, n = 2; P4, n = 4. _Endosialin_[−/−]: P2, n = 2; P3, n = 3; P4, n = 4.

collagen IV–positive empty sleeves (Figure 7E arrowheads). In keeping with our earlier observations (Figure 5A), apoptotic endothelial cells were predominantly found in the small vessels around the arteries and in the more mature remodeling plexus proximal to the optic disc, where selective vessel regression is most prominent at P4 and P5. There was a significant reduction in the number of apoptotic endothelial cells in _Endosialin_[−/−] retinas at P4 and a clear trend toward reduction at P5 (Figure 7E), demonstrating a role for endosialin in the functional cooperation in vivo of pericytes and endothelial cells to regulate vessel density.

Discussion

Compared with the abundant information on angiogenic sprouting, the processes and players involved in vascular pruning during the remodeling phase of vascular network formation remain relatively

obscure.[41] The study presented here provides a new perspective on the mechanisms that regulate vascular pruning by presenting the first evidence that pericytes can actively promote selective vessel destabilization and regression in vivo. This has important implications in the understanding of pericyte biology, because until now pericyte investment has been regarded as promoting rather than antagonizing vessel survival and stabilization. Moreover, our data indicate that this role of pericytes in selective vessel pruning occurs in both physiologic and pathologic angiogenesis and provides a mechanistic explanation for the aberrant vessel density observed in the present study and in previous studies[25,37] in tumors grown in _Endosialin_[−/−] mice.

Two main mechanisms for promoting endothelial cell apoptosis in the remodeling vasculature have been reported: (1) down-regulation of VEGF after increased tissue oxygenation results in apoptosis of newly established vessels that are still dependent on VEGF for their survival[31,33] and (2) recruitment of cytotoxic
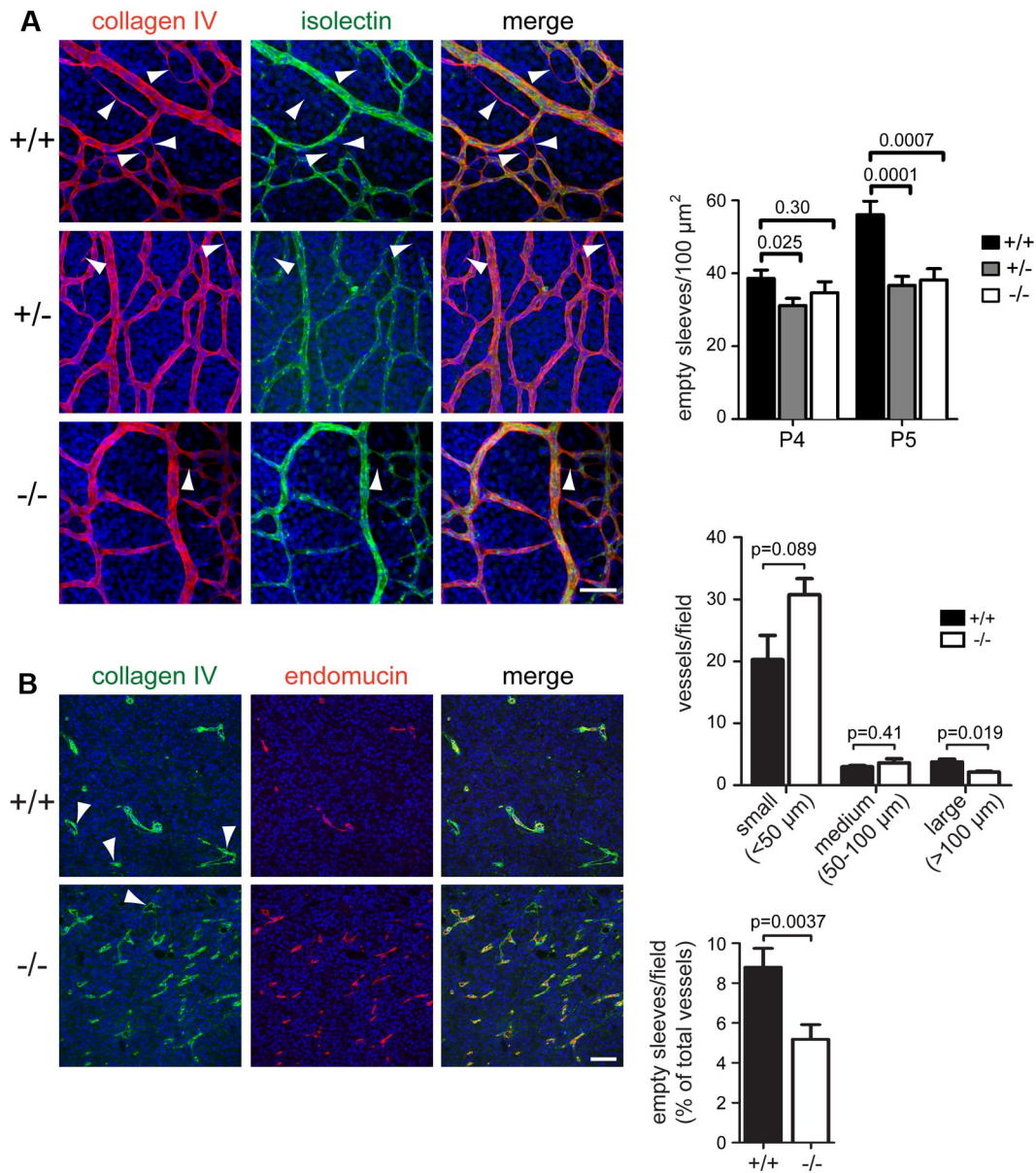
Figure 5. Loss of *Endosialin* leads to a defect in selective vessel regression. (A) Retinas from littermate *Endosialin*^{+/+}, *Endosialin*^{+/−}, and *Endosialin*^{−/−} C57BL/6 mice were stained with FITC–isolectin B4 (green), the basement membrane marker collagen IV (red), and DAPI (blue). Left panel, representative confocal images from P5 retinas. Arrowheads show collagen IV–positive, isolectin B4–negative empty sleeves indicating vessel regression. Scale bar indicates 25 μm. Right panels, quantification of mean number of empty sleeves ± SEM. *Endosialin*^{+/+}: P4, n = 4; P5, n = 7. *Endosialin*^{+/−}: P4, n = 5; P5, n = 5. *Endosialin*^{−/−}: P4, n = 3; P5, n = 3. (B) B16-F0 melanoma xenografts grown for 14 days in *Endosialin*^{+/+} or *Endosialin*^{−/−} mice (mean tumor diameter, 7.1 mm) were formalin fixed, paraffin embedded, and sections were stained for collagen IV (green) and endomucin (red). Nuclei were counterstained with DAPI (blue). Arrowheads show collagen IV–positive, endomucin-negative empty sleeves. Scale bar indicates 100 μm. Graphs show the distribution of vessel size and the number of empty sleeves as a percentage of total vessels ± SEM. *Endosialin*^{+/+}: n = 3; *Endosialin*^{−/−}: n = 3.

T lymphocytes resulting in Fas ligand–mediated endothelial cell killing.[34] Our in vitro and in vivo data demonstrate that endosialin expressed on pericytes can promote endothelial cell apoptosis. This may occur via endosialin bound to the vascular basement membrane directly disrupting endothelial cell adhesion to the matrix. Alternatively, matrix-bound endosialin may impair the cross-talk between endothelial integrins and VEGFR2, leading to the attenuation of VEGF signaling and subsequent endothelial cell apoptosis. The issue of whether the endothelial cell apoptosis leads to vessel regression or if vessel regression leads to apoptosis has been discussed in the literature and both scenarios are considered possible.[42] In addition, it has been demonstrated recently that embryonic fibroblasts expressing endosialin with a truncated cytoplasmic domain are impaired in their ability to bind U937 monocytes.[43] Therefore, endosialin may also modulate selective vessel pruning via its ability to promote localized leukocyte recruitment.

Very little is known about the mechanisms by which particular vessels are selected for pruning while adjacent vessels remain patent. Our data presented herein demonstrate that endosialin plays a role in this process and further suggest that the activity of endosialin could be restricted to selected vessels by the regulated availability of its ligand. It has been demonstrated previously in cell-free assays that endosialin can bind to the extracellular matrix components fibronectin and collagen IV (but not to vitronectin or laminin),[38] and to the tumor cell–secreted component Mac-2
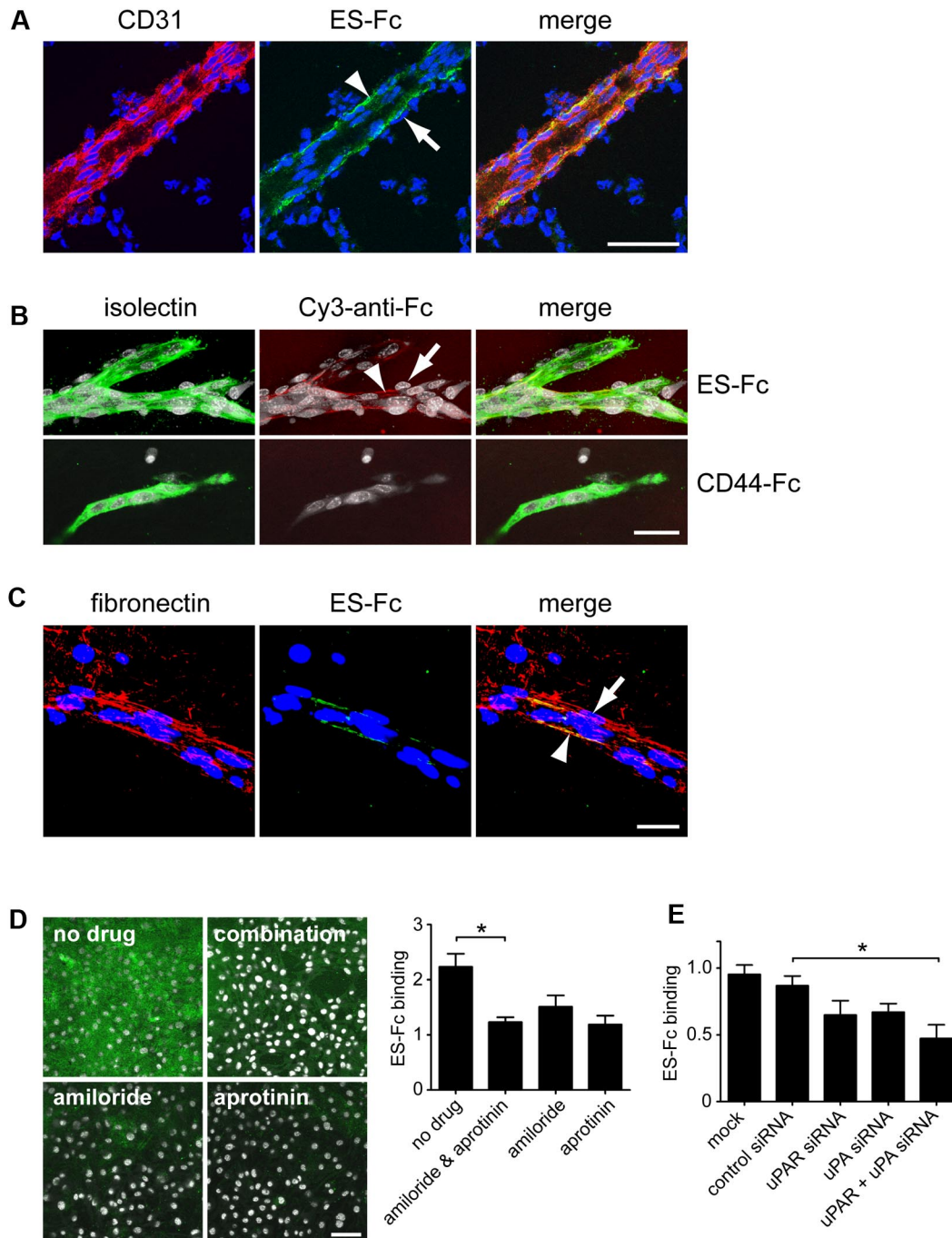
Figure 6. Endosialin binds to the vascular basement membrane in vivo. (A) Cryosections of embryonic day 15 mouse brain were incubated with mouse ES-Fc overnight at 4°C. The following day, sections were stained with FITC–anti-Fc (green) and anti-CD31, followed by Alexa Fluor 555–anti-rat IgG (red). Nuclei were counterstained with DAPI (blue). Arrowheads indicate ES-Fc binding associated with the abluminal side of the endothelial cells but not with the adjacent pericytes (arrows). Scale bar indicates 50 μm. (B) Aortic ring outgrowths from wild-type 129/SvJ mice were cultured for 6 days and then stained with ES-Fc or CD44-Fc for 1 hour at 37°C. After fixation, cultures were stained with Cy3–anti-Fc (red) and FITC–isolectin B4 (green). Nuclei were counterstained with DAPI (white). Arrowheads indicate ES-Fc binding associated with the abluminal side of the endothelial cells but not with the adjacent pericytes (arrows). Scale bar indicates 50 μm. (C) Aortic ring outgrowths were incubated with ES-Fc as described in panel B. After fixation, cultures were stained with FITC–anti-Fc (green) and antifibronectin, followed by Alexa Fluor 555–anti–rabbit Ig (red). Nuclei were counterstained with DAPI (blue). Arrowhead indicates colocalization with fibronectin on the abluminal surface of the endothelial cells. Arrow indicates lack of colocalization with fibronectin associated with the basement membrane surrounding the pericytes. Scale bar indicates 25 μm. (D) Immortalized mouse skin endothelial cells (sEND) cells were cultured for 2 days on coverslips in the presence of no drug, amiloride, and/or aprotinin. Cells were incubated with ES-Fc for 1 hour at 37°C, fixed, and stained with FITC–anti-Fc (green). Nuclei were counterstained with DAPI (white). Scale bar indicates 50 μm. Representative images are shown. Data shows quantification of ES-Fc binding from 3 independent experiments ± SEM. *$P < .05$. (E) sEND cells were either mock transfected or transfected with control siRNA, uPAR siRNA, uPA siRNA, or uPA plus uPAR siRNAs. Forty-eight hours after transfection, cells were incubated with ES-Fc as described in panel D. Data show quantification of ES-Fc binding from 3 independent experiments ± SEM. *$P < .05$.

BP/90K.[44] In the present study, we show that endosialin binding in vivo and in ex vivo samples is restricted to the endothelial cell basement membrane. No binding was detected to the basement membrane covering the pericytes despite abundant deposition of both collagen IV and fibronectin throughout the vascular basement membrane, demonstrating that endosialin does not bind universally to fibronectin or collagen IV, or indeed other known basement membrane components. Therefore, in vivo, either endosialin binds
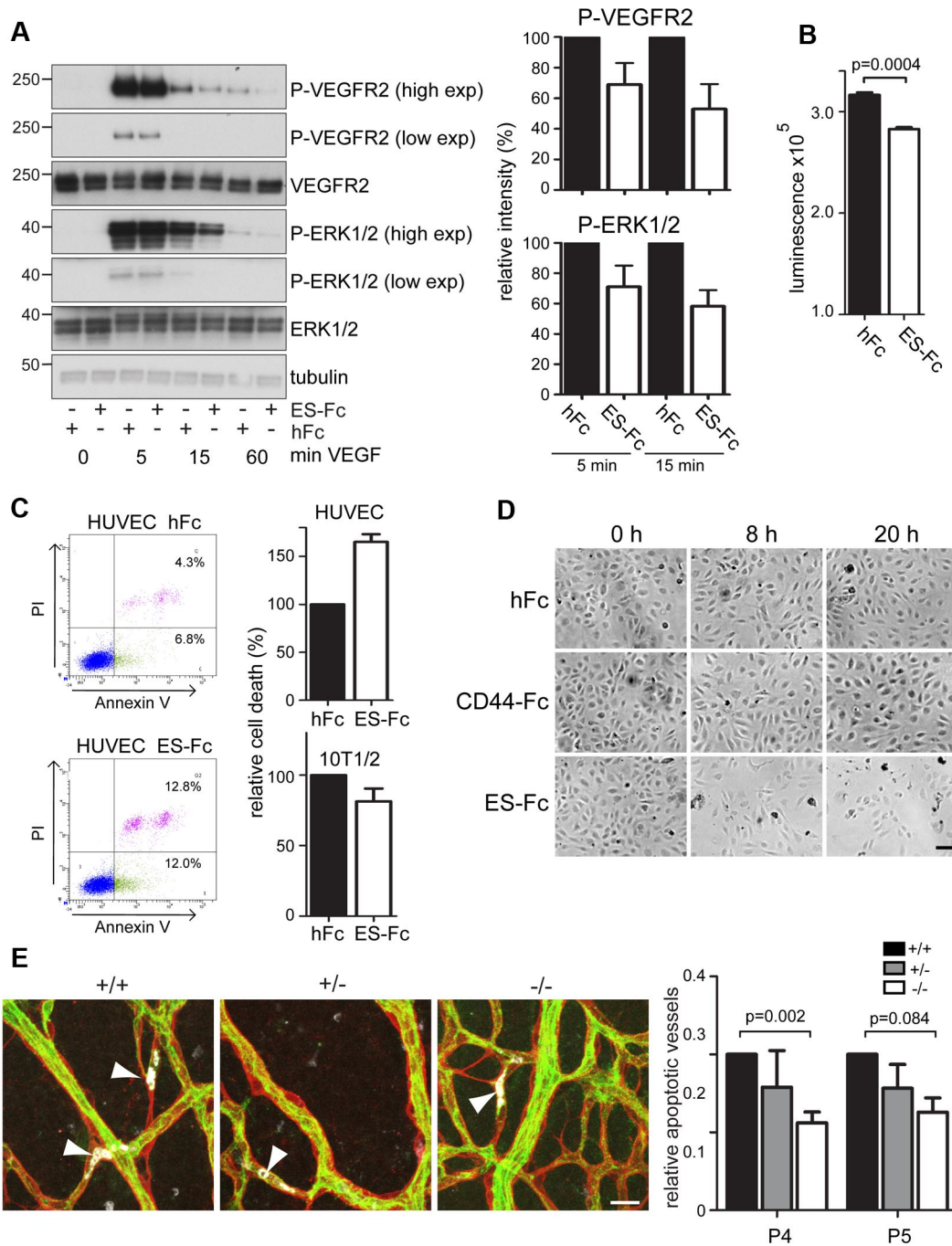
Figure 7. Endosialin modulates VEGF-A signaling and promotes endothelial cell apoptosis. (A) HUVECs cultured on ES-Fc- or hFc-coated plates were stimulated with VEGF-A, lysed, and subject to immunoblotting using the indicated Abs. Antitubulin mAb was used as a loading control. Molecular size markers are in kilodaltons. High- and low-exposure blots are shown. Quantification of the band intensities are from 3 independent experiments ± SEM. Data are normalized to the loading control and are shown relative to the hFc control at each time point. (B) HUVECs (4×10^3) were cultured on ES-Fc- or hFc-coated 96-well plates for 24 hours. Media were replaced with serum-free media supplemented with 20 ng/mL of VEGF-A and cells were cultured for a further 24 hours. Cell viability was measured using the CellTiter-Glo assay. Data shown are from 1 of 3 representative experiments with n = 3 samples ± SEM. (C) HUVECs or 10T1/2 cells incubated for 3 hours with VEGF-A in the presence of ES-Fc or hFc were stained with FITC–annexin V and/or propidium iodide (PI) and subjected to FACS analysis. Representative HUVEC FACS profiles are shown. Graph shows annexin V–positive/PI-positive, and annexin V–positive/PI-negative cells in the presence of ES-Fc from 2 independent experiments ± SD relative to the hFc control. (D) Phase-contrast images of HUVECs cultured in medium containing VEGF-A in the presence of hFc, ES-Fc, or CD44-Fc for 0, 8, and 20 hours. Scale bar indicates 100 μm. (E) Retinas from *Endosialin*^{+/+}, *Endosialin*^{+/−}, and *Endosialin*^{−/−} C57BL/6 mice were stained for collagen IV (red), activated caspase-3 (white), and FITC–isolectin B4 (green). Images show activated caspase-3–positive endothelial cells (arrowheads) associated with collagen IV empty sleeves in P4 retinas. Scale bar indicates 20 μm. Graph shows relative number of apoptotic (activated caspase-3–positive) vessels ± SEM. *Endosialin*^{+/+}: P4, n = 7; P5, n = 2; *Endosialin*^{+/−}: P4, n = 6; P5, n = 5; *Endosialin*^{−/−}: P4, n = 11; P5, n = 4.

to an endothelial cell–specific basement membrane component or modification of the vascular basement membrane by endothelial cells is required for endosialin binding. Intriguingly, the endosialin-binding site in fibronectin is located in the N-terminal 70-kDa domain[38] and we show here that binding to the endothelial cell

extracellular matrix requires endothelial cell uPA/uPAR activity. uPA/uPAR converts plasminogen to plasmin, which cleaves fibronectin directly within the 70-kDa fibronectin fragment.[45] Such proteolytic processing could localize endosialin activity and suggests a potential mechanism by which pericytes and endothelial

cells work cooperatively to fine-tune the balance between vessel regression and vessel stabilization. There is precedence for sprouting angiogenesis in vivo being regulated by the differential expression and processing of basement membrane components and by uPAR expression in retinal endothelial tip cells.[46,47] Although the molecular mechanisms remain unclear, uPAR processing of basement membrane components has been proposed to facilitate sprout migration, growth, and/or gene expression. uPAR deficiency causes defects in neovascularization during oxygen-induced retinopathy[48] and has been shown to play a key role in tumor angiogenesis.[49] However, lack of uPAR alone does not impair postnatal retinal angiogenesis,[48] highlighting the fact that the precise combination of proteases required remains to be determined. Nevertheless, the data of del Toro et al[46] and the present results support a model in which endothelial cell uPAR activity functions in both sprouting angiogenesis and vascular pruning to regulate vascular patterning.

Interactions between pericytes, endothelial cells, and the basement membrane change as vessels mature and new basement membrane is deposited and remodeled.[6,7,40] In the developing postnatal retina, these maturing vessels eventually become fully stabilized and switch to a nonplastic phenotype covered by mature pericytes that function to promote vessel survival. A better understanding of the plasticity and maturity of blood vessels, and in particular the mechanisms involved in vascular pruning, is important for the implementation of therapies designed to stimulate vascular network formation and inhibit excessive networks. For example, in regenerative medicine, tissue engineering, and the treatment of various ischemic diseases, the ability to promote vessel plasticity selectively is necessary for the formation of a functional, hierarchical vascular network in vivo. Similarly, in tumors, it may be desirable to provide a window of "normalized" vasculature to allow efficient delivery of therapeutics followed by the subsequent reversion of mature vessels to a more plastic state with increased responsiveness to VEGF blockade. This is exemplified in a recent study demonstrating in melanoma patients and a corresponding murine model that the level of perivascular differentiation, which influences the stabilization of the tumor vessels, governed the response to antiangiogenic therapy.[50] The results of the present study highlight the potential to exploit the targeting of endosialin and other regulators of vascular pruning as therapeutic strategies to promote vessel stabilization in some pathologies or to enforce vascular regression in others.

Authorship

Contribution: N.S., M.A., and A.v.W. performed the research and analyzed the data; S.L., D.L.H., and C.D.B. contributed vital reagents; N.S., I.J.H., H.Y., and C.M.I. designed the research and analyzed the data; and all authors contributed to writing the manuscript.

Conflict-of-interest disclosure: The authors declare no competing financial interests.

The current affiliation for N.S. is Institute of Virology, Technische Universität München/Helmholtz Zentrum München, Munich, Germany. The current affiliation for I.J.H. is The Netherlands Cancer Institute, Amsterdam, The Netherlands.

Correspondence: Clare M. Isacke, Breakthrough Breast Cancer Research Centre, Institute of Cancer Research, 237 Fulham Road, London SW3 6JB, United Kingdom; e-mail, clare.isacke@icr.ac.uk.

References

1. Adams RH, Alitalo K. Molecular regulation of angiogenesis and lymphangiogenesis. *Nat Rev Mol Cell Biol.* 2007;8(6):464-478.

2. Carmeliet P. Angiogenesis in life, disease and medicine. *Nature.* 2005;438(7070):932-936.

3. Phng LK, Gerhardt H. Angiogenesis: a team effort coordinated by notch. *Dev Cell.* 2009;16(2):196-208.

4. Lee HJ, Ahn BJ, Shin MW, Jeong JW, Kim JH, Kim KW. Ninjurin1 mediates macrophage-induced programmed cell death during early ocular development. *Cell Death Differ.* 2009;16(10):1395-1407.

5. Rao S, Lobov IB, Vallance JE, et al. Obligatory participation of macrophages in an angiopoietin 2-mediated cell death switch. *Development.* 2007;134(24):4449-4458.

6. Gaengel K, Genove G, Armulik A, Betsholtz C. Endothelial-mural cell signaling in vascular development and angiogenesis. *Arterioscler Thromb Vasc Biol.* 2009;29(5):630-638.

7. Bergers G, Song S. The role of pericytes in blood-vessel formation and maintenance. *Neuro Oncol.* 2005;7(4):452-464.

8. Armulik A, Genove G, Betsholtz C. Pericytes: developmental, physiological, and pathological perspectives, problems, and promises. *Dev Cell.* 2011;21(2):193-215.

9. Augustin HG, Koh GY, Thurston G, Alitalo K. Control of vascular morphogenesis and homeostasis through the angiopoietin-Tie system. *Nat Rev Mol Cell Biol.* 2009;10(3):165-177.

10. Yancopoulos GD, Davis S, Gale NW, Rudge JS, Wiegand SJ, Holash J. Vascular-specific growth factors and blood vessel formation. *Nature.* 2000; 407(6801):242-248.

11. Benjamin LE, Hemo I, Keshet E. A plasticity window for blood vessel remodelling is defined by pericyte coverage of the preformed endothelial network and is regulated by PDGF-B and VEGF. *Development.* 1998;125(9):1591-1598.

12. Enge M, Bjarnegard M, Gerhardt H, et al. Endothelium-specific platelet-derived growth factor-B ablation mimics diabetic retinopathy. *EMBO J.* 2002;21(16):4307-4316.

13. Hammes HP, Lin J, Renner O, et al. Pericytes and the pathogenesis of diabetic retinopathy. *Diabetes.* 2002;51(10):3107-3112.

14. Bondjers C, Kalen M, Hellstrom M, et al. Transcription profiling of platelet-derived growth factor-B-deficient mouse embryos identifies RGS5 as a novel marker for pericytes and vascular smooth muscle cells. *Am J Pathol.* 2003; 162(3):721-729.

15. Fruttiger M. Development of the mouse retinal vasculature: angiogenesis versus vasculogenesis. *Invest Ophthalmol Vis Sci.* 2002;43(2):522-527.

16. Ozerdem U, Grako KA, Dahlin-Huppe K, Monosov E, Stallcup WB. NG2 proteoglycan is expressed exclusively by mural cells during vascular morphogenesis. *Dev Dyn.* 2001;222(2):218-227.

17. Witmer AN, van Blijswijk BC, van Noorden CJ, Vrensen GF, Schlingemann RO. In vivo angiogenic phenotype of endothelial cells and pericytes induced by vascular endothelial growth factor-A. *J Histochem Cytochem.* 2004;52(1):39-52.

18. MacFadyen J, Savage K, Wienke D, Isacke CM. Endosialin is expressed on stromal fibroblasts and CNS pericytes in mouse embryos and is downregulated during development. *Gene Expr Patterns.* 2007;7(3):363-369.

19. MacFadyen JR, Haworth O, Roberston D, et al. Endosialin (TEM1, CD248) is a marker of stromal fibroblasts and is not selectively expressed on tumour endothelium. *FEBS Lett.* 2005;579(12): 2569-2575.

20. Simonavicius N, Robertson D, Bax DA, Jones C, Huijbers IJ, Isacke CM. Endosialin (CD248) is a marker of tumor-associated pericytes in high-grade glioma. *Mod Pathol.* 2008;21(3):308-315.

21. Bagley RG, Honma N, Weber W, et al. Endosialin/TEM 1/CD248 is a pericyte marker of embryonic and tumor neovascularization. *Microvasc Res.* 2008;76(3):180-188.

22. Christian S, Winkler R, Helfrich I, et al. Endosialin (Tem1) is a marker of tumor-associated myofibroblasts and tumor vessel-associated mural cells. *Am J Pathol.* 2008;172(2):486-494.

23. Rupp C, Dolznig H, Puri C, et al. Mouse endosialin, a C-type lectin-like cell surface receptor: expression during embryonic development and induction in experimental cancer neoangiogenesis. *Cancer Immun.* 2006;6:10.

24. Mason JC, Yarwood H, Sugars K, Morgan BP, Davies KA, Haskard DO. Induction of decay-accelerating factor by cytokines or the membrane-attack complex protects vascular endothelial cells against complement deposition. *Blood.* 1999; 94(5):1673-1682.

25. Nanda A, Karim B, Peng Z, et al. Tumor endothelial marker 1 (Tem1) functions in the growth and progression of abdominal tumors. *Proc Natl Acad Sci U S A.* 2006;103(9):3351-3356.

26. Pitulescu ME, Schmidt I, Benedito R, Adams RH. Inducible gene targeting in the neonatal vasculature and analysis of retinal angiogenesis in mice. *Nat Protoc.* 2010;5(9):1518-1534.

27. Nicosia RF, Ottinetti A. Growth of microvessels in serum-free matrix culture of rat aorta. A quantitative assay of angiogenesis in vitro. *Lab Invest.* 1990;63(1):115-122.

28. Peach RJ, Hollenbaugh D, Stamenkovic I, Aruffo A. Identification of hyaluronic acid binding sites in the extracellular domain of CD44. *J Cell Biol.* 1993;122(1):257-264.

29. Fruttiger M. Development of the retinal vasculature. *Angiogenesis.* 2007;10(2):77-88.

30. Virgintino D, Girolamo F, Errede M, et al. An intimate interplay between precocious, migrating pericytes and endothelial cells governs human fetal brain angiogenesis. *Angiogenesis.* 2007; 10(1):35-45.

31. Alon T, Hemo I, Itin A, Pe'er J, Stone J, Keshet E. Vascular endothelial growth factor acts as a survival factor for newly formed retinal vessels and has implications for retinopathy of prematurity. *Nat Med.* 1995;1(10):1024-1028.

32. Baffert F, Le T, Sennino B, et al. Cellular changes in normal blood capillaries undergoing regression after inhibition of VEGF signaling. *Am J Physiol Heart Circ Physiol.* 2006;290(2):H547-559.

33. Inai T, Mancuso M, Hashizume H, et al. Inhibition of vascular endothelial growth factor (VEGF) signaling in cancer causes loss of endothelial fenestrations, regression of tumor vessels, and appearance of basement membrane ghosts. *Am J Pathol.* 2004;165(1):35-52.

34. Ishida S, Yamashiro K, Usui T, et al. Leukocytes mediate retinal vascular remodeling during development and vaso-obliteration in disease. *Nat Med.* 2003;9(6):781-788.

35. Kubota Y, Takubo K, Shimizu T, et al. M-CSF inhibition selectively targets pathological angiogenesis and lymphangiogenesis. *J Exp Med.* 2009; 206(5):1089-1102.

36. Phng LK, Potente M, Leslie JD, et al. Nrarp coordinates endothelial Notch and Wnt signaling to control vessel density in angiogenesis. *Dev Cell.* 2009;16(1):70-82.

37. Carson-Walter EB, Winans BN, Whiteman MC, et al. Characterization of TEM1/endosialin in human and murine brain tumors. *BMC Cancer.* 2009;9: 417.

38. Tomkowicz B, Rybinski K, Foley B, et al. Interaction of endosialin/TEM1 with extracellular matrix proteins mediates cell adhesion and migration. *Proc Natl Acad Sci U S A.* 2007;104(46):17965-17970.

39. Davis GE, Senger DR. Endothelial extracellular

matrix: biosynthesis, remodeling, and functions during vascular morphogenesis and neovessel stabilization. *Circ Res.* 2005;97(11):1093-1107.

40. Kalluri R. Basement membranes: structure, assembly and role in tumour angiogenesis. *Nat Rev Cancer.* 2003;3(6):422-433.

41. Benjamin LE. The controls of microvascular survival. *Cancer Metastasis Rev.* 2000;19(1-2):75-81.

42. Im E, Kazlauskas A. New insights regarding vessel regression. *Cell Cycle.* 2006;5(18):2057-2059.

43. Maia M, de Vriese A, Janssens T, et al. CD248 and its cytoplasmic domain: a therapeutic target for arthritis. *Arthritis Rheum.* 2010;62(12):3595-3606.

44. Becker R, Lenter MC, Vollkommer T, et al. Tumor stroma marker endosialin (Tem1) is a binding partner of metastasis-related protein Mac-2 BP/ 90K. *FASEB J.* 2008;22(8):3059-3067.

45. Pankov R, Yamada KM. Fibronectin at a glance. *J Cell Sci.* 2002;115(20):3861-3863.

46. del Toro R, Prahst C, Mathivet T, et al. Identification and functional analysis of endothelial tip cell-enriched genes. *Blood.* 2010;116(19):4025-4033.

47. Stenzel D, Franco CA, Estrach S, et al. Endothelial basement membrane limits tip cell formation by inducing Dll4/Notch signalling in vivo. *EMBO Rep.* 2011;12(11):1135-1143.

48. McGuire PG, Jones TR, Talarico N, Warren E, Das A. The urokinase/urokinase receptor system in retinal neovascularization: inhibition by A6 suggests a new therapeutic target. *Invest Ophthalmol Vis Sci.* 2003;44(6):2736-2742.

49. Blasi F, Carmeliet P. uPAR: a versatile signalling orchestrator. *Nat Rev Mol Cell Biol.* 2002;3(12): 932-943.

50. Helfrich I, Scheffrahn I, Bartling S, et al. Resistance to antiangiogenic therapy is directed by vascular phenotype, vessel stabilization, and maturation in malignant melanoma. *J Exp Med.* 2010;207(3):491-503.